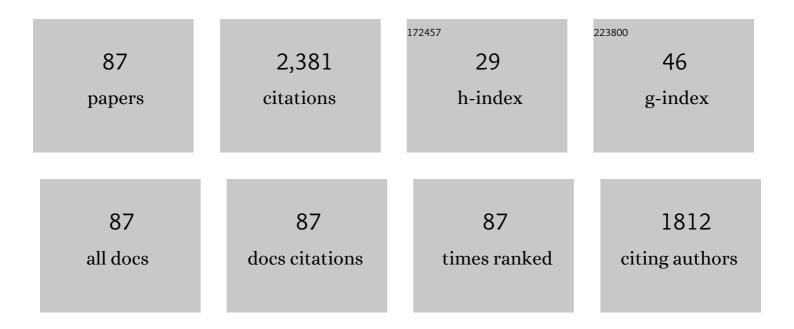
List of Publications by Year in descending order

Source: https://exaly.com/author-pdf/1286716/publications.pdf Version: 2024-02-01



#	Article	IF	CITATIONS
1	Migration and abiotic transformation of estrone (E1) and estrone-3-sulfate (E1-3S) during soil column transport. Environmental Geochemistry and Health, 2022, 44, 911-924.	3.4	2
2	Effects of low impact development on the stormwater runoff and pollution control. Science of the Total Environment, 2022, 805, 150404.	8.0	25
3	Z-scheme Ag3PO4@polyaniline core-shell nanocomposite with high visible light photocatalytic performance for Microcystis aeruginosa inactivation. Chemical Engineering Journal, 2022, 427, 132005.	12.7	30
4	Magnetically separable ZnFe2O4/Ag3PO4/g-C3N4 photocatalyst for inactivation of Microcystis aeruginosa: Characterization, performance and mechanism. Journal of Hazardous Materials, 2022, 421, 126703.	12.4	60
5	Sono-photo hybrid process for the synergistic degradation of levofloxacin by FeVO4/BiVO4: Mechanisms and kinetics. Environmental Research, 2022, 204, 112032.	7.5	46
6	Enhanced degradation capability of white-rot fungi after short-term pre-exposure to silver ion: Performance and selectively antimicrobial mechanisms. Science of the Total Environment, 2022, 818, 151672.	8.0	2
7	Spatio-temporal variations of salinity and analysis of desalination factors in a Chinese coastal storage reservoir. Chemical Engineering Research and Design, 2022, 159, 26-35.	5.6	0
8	Sonophotocatalytic degradation of 17î²-estradiol by Er3+-CdS/MoS2: The role and transformation of reactive oxygen species. Journal of Cleaner Production, 2022, 333, 130203.	9.3	9
9	Photocatalytic inactivation of algae in a fluidized bed photoreactor with an external magnetic field. Journal of Environmental Management, 2022, 307, 114552.	7.8	1
10	High removal of nitrogen and phosphorus from black-odorous water using a novel aeration-adsorption system. Environmental Chemistry Letters, 2022, 20, 2243-2251.	16.2	12
11	Oxidation-enhanced ferric coagulation for alleviating ultrafiltration membrane fouling by algal organic matter: A comparison of moderate and strong oxidation. Algal Research, 2022, 63, 102652.	4.6	14
12	Membrane distillation treatment of landfill leachate: Characteristics and mechanism of membrane fouling. Separation and Purification Technology, 2022, 289, 120787.	7.9	28
13	Microbial community and nitrogen transformation pathway in bioretention system for stormwater treatment in response to formulated soil medium. Chemical Engineering Research and Design, 2022, 161, 594-602.	5.6	8
14	Photocatalytic membrane for in situ enhanced removal of semi-volatile organic compounds in membrane distillation under visible light. Separation and Purification Technology, 2022, 292, 121068.	7.9	16
15	An innovative S-scheme AgCl/MIL-100(Fe) heterojunction for visible-light-driven degradation of sulfamethazine and mechanism insight. Journal of Hazardous Materials, 2022, 435, 129061.	12.4	45
16	Metal–organic-framework-based photocatalysts for microorganism inactivation: a review. Catalysis Science and Technology, 2022, 12, 3767-3777.	4.1	13
17	Porous self-floating 3D Ag2O/g-C3N4 hydrogel and photocatalytic inactivation of Microcystis aeruginosa under visible light. Chemical Engineering Journal, 2021, 404, 126509.	12.7	60
18	Effect of biopolymers and humic substances on gypsum scaling and membrane wetting during membrane distillation. Journal of Membrane Science, 2021, 617, 118638.	8.2	78

#	Article	IF	CITATIONS
19	Double photoelectron-transfer mechanism in Agâ <sup>°°</sup> AgCl/WO3/g-C3N4 photocatalyst with enhanced visible-light photocatalytic activity for trimethoprim degradation. Journal of Hazardous Materials, 2021, 403, 123964.	12.4	116
20	Fabrication of heterostructured Ag/AgCl@g-C3N4@UIO-66(NH2) nanocomposite for efficient photocatalytic inactivation of Microcystis aeruginosa under visible light. Journal of Hazardous Materials, 2021, 404, 124062.	12.4	113
21	Membrane fouling control by UV/persulfate in tertiary wastewater treatment with ultrafiltration: A comparison with UV/hydroperoxide and role of free radicals. Separation and Purification Technology, 2021, 257, 117877.	7.9	27
22	Algae-laden water treatment with ultrafiltration: effects of moderate oxidation by Fe( <scp>ii</scp> )/permanganate on hydraulically irreversible fouling and deposition of iron and manganese oxides. Environmental Science: Water Research and Technology, 2021, 7, 122-133.	2.4	6
23	Impact of Extracellular Polymeric Substance in the Inactivation of Harmful Algae by Ag <sub>2</sub> 0/gâ€C <sub>3</sub> N <sub>4</sub> under Visible Light. Particle and Particle Systems Characterization, 2021, 38, 2000272.	2.3	7
24	Water Quality-Based Double-Gates Control Strategy for Combined Sewer Overflows Pollution Control. Water (Switzerland), 2021, 13, 529.	2.7	6
25	Enhanced photocatalytic performance of Z-scheme N-doped Ag2CO3/GO (AGON) for microcystin-LR remediation under visible light. Journal of Water Process Engineering, 2021, 39, 101882.	5.6	8
26	Optimization of remedial nano-agent and its effect on dominant algal species succession in eutrophic water body. Journal of Environmental Management, 2021, 281, 111884.	7.8	3
27	Hydrologic characteristics and nitrogen removal performance by different formulated soil medium of bioretention system. Journal of Cleaner Production, 2021, 290, 125873.	9.3	15
28	Efficient integration of plasmonic Ag/AgCl with perovskite-type LaFeO3: Enhanced visible-light photocatalytic activity for removal of harmful algae. Journal of Hazardous Materials, 2021, 409, 125018.	12.4	66
29	Mussel-Inspired Immobilization of Photocatalysts with Synergistic Photocatalytic–Photothermal Performance for Water Remediation. ACS Applied Materials & Interfaces, 2021, 13, 31066-31076.	8.0	20
30	Integration of seeding- and heating-induced crystallization with membrane distillation for membrane gypsum scaling and wetting control. Desalination, 2021, 511, 115115.	8.2	27
31	A citrate-loaded nano-zero-valent iron heterogeneous Fenton system for steroid estrogens degradation under different acidity levels: The effects and mechanisms. Chemical Engineering Journal, 2021, 421, 129967.	12.7	7
32	Recyclable self-floating A-GUN-coated foam as effective visible-light-driven photocatalyst for inactivation of Microcystis aeruginosa. Journal of Hazardous Materials, 2021, 419, 126407.	12.4	32
33	Self-floating photocatalytic hydrogel for efficient removal of Microcystis aeruginosa and degradation of microcystins-LR. Chemosphere, 2021, 284, 131283.	8.2	11
34	Evaluation of applying membrane distillation for landfill leachate treatment. Desalination, 2021, 520, 115358.	8.2	33
35	Enhancing the antifouling and rejection properties of PVDF membrane by Ag3PO4-GO modification. Science of the Total Environment, 2021, 801, 149611.	8.0	21
36	Metagenomics reveals functional species and microbial mechanisms of an enriched thiosulfate-driven denitratation consortia. Bioresource Technology, 2021, 341, 125916.	9.6	10

#	Article	IF	CITATIONS
37	Membrane Distillation for Wastewater Treatment: A Mini Review. Water (Switzerland), 2021, 13, 3480.	2.7	15
38	Visible-light-driven photocatalytic degradation of naproxen by Bi-modified titanate nanobulks: Synthesis, degradation pathway and mechanism. Journal of Photochemistry and Photobiology A: Chemistry, 2020, 386, 112108.	3.9	26
39	Fast photocatalytic inactivation of Microcystis aeruginosa by metal-organic frameworks under visible light. Chemosphere, 2020, 239, 124721.	8.2	37
40	Stable Ag2O/g-C3N4 p-n heterojunction photocatalysts for efficient inactivation of harmful algae under visible light. Applied Catalysis B: Environmental, 2020, 265, 118610.	20.2	128
41	Photocatalytic inactivation of harmful algae and degradation of cyanotoxins microcystin-LR using GO-based Z-scheme nanocatalysts under visible light. Chemical Engineering Journal, 2020, 392, 123767.	12.7	45
42	Characterizing the anthropogenic-induced trace elements in an urban aquatic environment: A source apportionment and risk assessment with uncertainty consideration. Journal of Environmental Management, 2020, 275, 111288.	7.8	15
43	Effect of residual commercial antiscalants on gypsum scaling and membrane wetting during direct contact membrane distillation. Desalination, 2020, 486, 114493.	8.2	39
44	Operating parameters optimization of combined UF/NF dual-membrane process for brackish water treatment and its application performance in municipal drinking water treatment plant. Journal of Water Process Engineering, 2020, 38, 101547.	5.6	15
45	Occurrence and risk assessment of steroid estrogens in environmental water samples: A five-year worldwide perspective. Environmental Pollution, 2020, 267, 115405.	7.5	57
46	Mussel-inspired polydopamine modification of polymeric membranes for the application of water and wastewater treatment: A review. Chemical Engineering Research and Design, 2020, 157, 195-214.	5.6	87
47	Simultaneous removal of harmful algal cells and toxins by a Ag2CO3-N:CO photocatalyst coating under visible light. Science of the Total Environment, 2020, 741, 140341.	8.0	38
48	Spatio-temporal distribution and transformation of 17α- and 17β-estradiol in sterilized soil: A column experiment. Journal of Hazardous Materials, 2020, 389, 122092.	12.4	13
49	Photocatalytic degradation of naproxen by a H <sub>2</sub> O <sub>2</sub> -modified titanate nanomaterial under visible light irradiation. Catalysis Science and Technology, 2019, 9, 4614-4628.	4.1	31
50	Photocatalytic Removal of Harmful Algae in Natural Waters by Ag/AgCl@ZIF-8 Coating under Sunlight. Catalysts, 2019, 9, 698.	3.5	14
51	Strategy of Rainwater Discharge in Combined Sewage Intercepting Manhole Based on Water Quality Control. Water (Switzerland), 2019, 11, 898.	2.7	6
52	Inactivation of harmful cyanobacteria by Ag/AgCl@ZIF-8 coating under visible light: Efficiency and its mechanisms. Applied Catalysis B: Environmental, 2019, 256, 117866.	20.2	63
53	Migration and transformation of nitrogen in bioretention system during rainfall runoff. Chemosphere, 2019, 232, 54-62.	8.2	48
54	Concentration decline in response to source shift of trace metals in Elbe River, Germany: A long-term trend analysis during 1998–2016. Environmental Pollution, 2019, 250, 511-519.	7.5	18

#	Article	IF	CITATIONS
55	The influence of heavy metals in road dust on the surface runoff quality: Kinetic, isotherm, and sequential extraction investigations. Ecotoxicology and Environmental Safety, 2019, 176, 270-278.	6.0	30
56	Tertiary treatment of secondary effluent using ultrafiltration for wastewater reuse: correlating membrane fouling with rejection of effluent organic matter and hydrophobic pharmaceuticals. Environmental Science: Water Research and Technology, 2019, 5, 672-683.	2.4	30
57	Inhibitory Effects of Cu2O/SiO2 on the Growth of Microcystis aeruginosa and Its Mechanism. Nanomaterials, 2019, 9, 1669.	4.1	10
58	Growth inhibition of harmful cyanobacteria by nanocrystalline Cu-MOF-74: Efficiency and its mechanisms. Journal of Hazardous Materials, 2019, 367, 529-538.	12.4	66
59	Removal of organics by combined process of coagulation–chlorination–ultrafiltration: optimization of overall operation parameters. Environmental Technology (United Kingdom), 2018, 39, 2703-2714.	2.2	1
60	Degradation of acetaminophen in aqueous solution under visible light irradiation by Bi-modified titanate nanomaterials: morphology effect, kinetics and mechanism. Catalysis Science and Technology, 2018, 8, 5906-5919.	4.1	33
61	Growth inhibition of <i>Microcystic aeruginosa</i> by metal–organic frameworks: effect of variety, metal ion and organic ligand. RSC Advances, 2018, 8, 35314-35326.	3.6	30
62	Growth Inhibition of Microcystis aeruginosa by Copperâ€based MOFs: Performance and Physiological Effect on Algal Cells. Applied Organometallic Chemistry, 2018, 32, e4600.	3.5	29
63	Rapid synthesis of Ag/AgCl@ZIF-8 as a highly efficient photocatalyst for degradation of acetaminophen under visible light. Chemical Engineering Journal, 2018, 351, 782-790.	12.7	163
64	Doping Ag/AgCl in zeolitic imidazolate framework-8 (ZIF-8) to enhance the performance of photodegradation of methylene blue. Chemosphere, 2018, 209, 44-52.	8.2	56
65	Optimization of Integrated Ultrafiltration Processes Using Response Surface Methodology. Environmental Engineering Science, 2017, 34, 165-176.	1.6	2
66	The influence of land use on source apportionment and risk assessment of polycyclic aromatic hydrocarbons in road-deposited sediment. Environmental Pollution, 2017, 229, 705-714.	7.5	35
67	Nitrogen removal from urban stormwater runoff by stepped bioretention systems. Ecological Engineering, 2017, 106, 340-348.	3.6	60
68	Removal of Cr (VI) from aqueous solutions by titanate nanomaterials synthesized via hydrothermal method. Canadian Journal of Chemical Engineering, 2017, 95, 717-723.	1.7	12
69	Synthesis and Characterization of the Optical Properties of Pt-TiO <sub>2</sub> Nanotubes. Journal of Nanomaterials, 2017, 2017, 1-9.	2.7	3
70	Influence of Membrane Materials and Operational Modes on the Performance of Ultrafiltration Modules for Drinking Water Treatment. International Journal of Polymer Science, 2016, 2016, 1-8.	2.7	7
71	Toward a better understanding of coagulation for dissolved organic nitrogen using polymeric zinc-iron-phosphate coagulant. Water Research, 2016, 100, 201-210.	11.3	42
72	Forecasting traffic-related nitrogen oxides within a street canyon by combining a genetic algorithm-back propagation artificial neural network and parametric models. Atmospheric Pollution Research, 2015, 6, 1087-1097.	3.8	7

#	Article	IF	CITATIONS
73	Response Surface Design for Optimization of Microcystis aeruginosa Removal by Ultrasonic Irradiation. Asian Journal of Chemistry, 2014, 26, 6967-6974.	0.3	о
74	Parameter Optimization of Ultrasound Technology for Algae Removal and its Application in Pengxi River of Three Gorges Reservoir. Asian Journal of Chemistry, 2014, 26, 1165-1170.	0.3	2
75	Influence factors in kinetics during removal of harmful algae by ultrasonic irradiation process. Desalination and Water Treatment, 2014, 52, 7317-7322.	1.0	1
76	DOM removal by flocculation process: Fluorescence excitation–emission matrix spectroscopy (EEMs) characterization. Desalination, 2014, 346, 38-45.	8.2	62
77	Response Surface Design for the Optimization of the Removal of Chlorella pyrenoidosa Low Frequency Ultrasonic Irradiation. Asian Journal of Chemistry, 2013, 25, 202-208.	0.3	4
78	Optimization of <i>Chlorella pyrenoidosa</i> Removal by Low Frequency Ultrasonic Irradiation Using Response Surface Design. Advanced Materials Research, 2011, 295-297, 1860-1865.	0.3	1
79	Analysis of the Water Intake Technology of Open-Lakes Water Source Heat Pump System in Chongqing. Advanced Materials Research, 2011, 250-253, 3168-3172.	0.3	Ο
80	The Application of Low-Frequency and Low-Power Ultrasound Algae Removal Technology in Pengxi River in Three Gorges Area. Advanced Materials Research, 2011, 295-297, 1852-1855.	0.3	0
81	The Characteristics of Lakes of Water Source Heat Pump Systems in Chongqing. , 2011, , .		Ο
82	Preventive inhibition mechanism of algae by ultrasound based on analysis of physiological characteristics. , 0, 68, 70-79.		8
83	Damaging effects of ultrasonic treatment on the photosynthetic system of Microcystis aeruginosa. , 0, 78, 350-359.		13
84	Impact of structure and morphology of titanate nanomaterials on Pb2+ adsorption in aqueous solution. , 0, 136, 306-319.		1
85	Response surface methodology for optimization of ZIF-8 synthesis conditions to enhance its removing capability for Pb(II) in aqueous solutions. , 0, 135, 141-156.		Ο
86	Effects of ultrasonic irradiation on organic matter of Microcystis aeruginosa cells. , 0, 129, 101-115.		1
87	Influence of H+ and Na+ ions on the morphology of titanate nanomaterial and its adsorption property of lead. , 0, 136, 320-331.		0